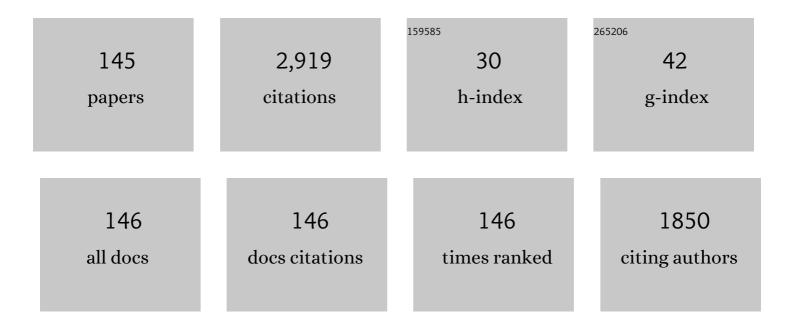
List of Publications by Year in descending order

Source: https://exaly.com/author-pdf/1423817/publications.pdf Version: 2024-02-01



#	Article	IF	CITATIONS
1	Separation of lithium and cobalt from waste lithium-ion batteries via bipolar membrane electrodialysis coupled with chelation. Separation and Purification Technology, 2013, 113, 33-41.	7.9	101
2	Preparation of BTESE-derived organosilica membranes for catalytic membrane reactors of methylcyclohexane dehydrogenation. Journal of Membrane Science, 2014, 455, 375-383.	8.2	96
3	Gas permeation properties for organosilica membranes with different Si/C ratios and evaluation of microporous structures. AICHE Journal, 2017, 63, 4491-4498.	3.6	65
4	Carbon dioxide recovery from carbonate solutions using bipolar membrane electrodialysis. Separation and Purification Technology, 2012, 101, 49-59.	7.9	64
5	Effect of firing temperature on the water permeability of SiO2–ZrO2 membranes for nanofiltration. Journal of Membrane Science, 2016, 497, 348-356.	8.2	59
6	Phase inversion/sintering-induced porous ceramic microsheet membranes for high-quality separation of oily wastewater. Journal of Membrane Science, 2020, 595, 117477.	8.2	59
7	Modified gasâ€ŧranslation model for prediction of gas permeation through microporous organosilica membranes. AICHE Journal, 2014, 60, 4199-4210.	3.6	52
8	A new recovery process of carbon dioxide from alkaline carbonate solution via electrodialysis. AICHE Journal, 2009, 55, 3286-3293.	3.6	50
9	Multilayered polyamide membranes by spray-assisted 2-step interfacial polymerization for increased performance of trimesoyl chloride (TMC)/m-phenylenediamine (MPD)-derived polyamide membranes. Journal of Membrane Science, 2013, 446, 504-512.	8.2	48
10	Graphene nanosheets supporting Ru nanoparticles with controlled nanoarchitectures form a high-performance catalyst for CO _x -free hydrogen production from ammonia. Journal of Materials Chemistry A, 2014, 2, 9185-9192.	10.3	47
11	Pervaporation dehydration of aqueous solutions of various types of molecules via organosilica membranes: Effect of membrane pore sizes and molecular sizes. Separation and Purification Technology, 2018, 207, 108-115.	7.9	47
12	Characterization and gas permeation properties of amorphous silica membranes prepared via plasma enhanced chemical vapor deposition. Journal of Membrane Science, 2013, 441, 45-53.	8.2	46
13	Role of Amine Type in CO2 Separation Performance within Amine Functionalized Silica/Organosilica Membranes: A Review. Applied Sciences (Switzerland), 2018, 8, 1032.	2.5	46
14	Energy-efficient separation of organic liquids using organosilica membranes via a reverse osmosis route. Journal of Membrane Science, 2020, 597, 117758.	8.2	46
15	Methylcyclohexane dehydrogenation for hydrogen production via a bimodal catalytic membrane reactor. AICHE Journal, 2015, 61, 1628-1638.	3.6	44
16	CO ₂ Permeation through Hybrid Organosilica Membranes in the Presence of Water Vapor. Industrial & Engineering Chemistry Research, 2014, 53, 6113-6120.	3.7	43
17	Pervaporation removal of methanol from methanol/organic azeotropes using organosilica membranes: Experimental and modeling. Journal of Membrane Science, 2020, 610, 118284.	8.2	43
18	Filtration of surfactant-stabilized oil-in-water emulsions with porous ceramic membranes: Effects of membrane pore size and surface charge on fouling behavior. Journal of Membrane Science, 2020, 610, 118210.	8.2	42

#	Article	IF	CITATIONS
19	Utilization of Bipolar Membrane Electrodialysis for the Removal of Boron from Aqueous Solution. Industrial & Engineering Chemistry Research, 2011, 50, 6325-6330.	3.7	41
20	SiO2-ZrO2 nanofiltration membranes of different Si/Zr molar ratios: Stability in hot water and acid/alkaline solutions. Journal of Membrane Science, 2017, 524, 700-711.	8.2	41
21	Atmospheric-pressure plasma-enhanced chemical vapor deposition of microporous silica membranes for gas separation. Journal of Membrane Science, 2017, 524, 644-651.	8.2	38
22	Microporous organosilica membranes for gas separation prepared via PECVD using different O/Si ratio precursors. Journal of Membrane Science, 2015, 489, 11-19.	8.2	37
23	Experimental and Theoretical Study on Small Gas Permeation Properties through Amorphous Silica Membranes Fabricated at Different Temperatures. Journal of Physical Chemistry C, 2014, 118, 20323-20331.	3.1	36
24	Pervaporation and vapor permeation characteristics of BTESE-derived organosilica membranes and their long-term stability in a high-water-content IPA/water mixture. Journal of Membrane Science, 2016, 498, 336-344.	8.2	36
25	Fabrication and CO2 permeation properties of amine-silica membranes using a variety of amine types. Journal of Membrane Science, 2017, 541, 447-456.	8.2	36
26	Tailoring the microstructure and permeation properties of bridged organosilica membranes via control of the bond angles. Journal of Membrane Science, 2019, 584, 56-65.	8.2	35
27	Gas permeation properties through Al-doped organosilica membranes with controlled network size. Journal of Membrane Science, 2014, 466, 246-252.	8.2	34
28	Pyrimidine-bridged organoalkoxysilane membrane for high-efficiency CO 2 transport via mild affinity. Separation and Purification Technology, 2017, 178, 232-241.	7.9	34
29	Atmospheric-pressure plasma-enhanced chemical vapor deposition of UV-shielding TiO2 coatings on transparent plastics. Materials Letters, 2018, 228, 479-481.	2.6	34
30	Bis(triethoxysilyl)ethane (BTESE)-derived silica membranes: pore formation mechanism and gas permeation properties. Journal of Sol-Gel Science and Technology, 2018, 86, 63-72.	2.4	33
31	UV-Protective TiO ₂ Thin Films with High Transparency in Visible Light Region Fabricated via Atmospheric-Pressure Plasma-Enhanced Chemical Vapor Deposition. ACS Applied Materials & Amp; Interfaces, 2018, 10, 42657-42665.	8.0	32
32	Fabrication of a layered hybrid membrane using an organosilica separation layer on a porous polysulfone support, and the application to vapor permeation. Journal of Membrane Science, 2014, 464, 140-148.	8.2	31
33	CO ₂ Fixation Process with Waste Cement Powder via Regeneration of Alkali and Acid by Electrodialysis: Effect of Operation Conditions. Industrial & Engineering Chemistry Research, 2015, 54, 6569-6577.	3.7	31
34	Network engineering of a BTESE membrane for improved gas performance via a novel pH-swing method. Journal of Membrane Science, 2016, 511, 219-227.	8.2	31
35	Fluorine-induced microporous silica membranes: Dramatic improvement in hydrothermal stability and pore size controllability for highly permeable propylene/propane separation. Journal of Membrane Science, 2018, 549, 111-119.	8.2	31
36	Development and gas permeation properties of microporous amorphous TiO2–ZrO2–organic composite membranes using chelating ligands. Journal of Membrane Science, 2014, 461, 96-105.	8.2	29

#	Article	IF	CITATIONS
37	Robust organosilica membranes for high temperature reverse osmosis (RO) application: Membrane preparation, separation characteristics of solutes and membrane regeneration. Journal of Membrane Science, 2015, 493, 515-523.	8.2	29
38	Improved thermal and oxidation stability of bis(triethoxysilyl)ethane (BTESE)-derived membranes, and their gas-permeation properties. Journal of Materials Chemistry A, 2018, 6, 23378-23387.	10.3	29
39	A CO ₂ fixation process with waste cement powder via regeneration of alkali and acid by electrodialysis. RSC Advances, 2014, 4, 19778-19788.	3.6	28
40	Preparation, characterization, and evaluation of TiO2-ZrO2 nanofiltration membranes fired at different temperatures. Journal of Membrane Science, 2018, 564, 691-699.	8.2	28
41	Tailoring Ultramicroporosity To Maximize CO ₂ Transport within Pyrimidine-Bridged Organosilica Membranes. ACS Applied Materials & Interfaces, 2019, 11, 7164-7173.	8.0	28
42	Insight into the pore tuning of triazine-based nitrogen-rich organoalkoxysilane membranes for use in water desalination. RSC Advances, 2014, 4, 23759-23769.	3.6	25
43	Fluorine Doping of Microporous Organosilica Membranes for Pore Size Control and Enhanced Hydrophobic Properties. ACS Omega, 2018, 3, 8612-8620.	3.5	25
44	Synthesis and characterization of a layered-hybrid membrane consisting of an organosilica separation layer on a polymeric nanofiltration membrane. Journal of Membrane Science, 2014, 472, 19-28.	8.2	24
45	Preparation of organosilica membranes on hydrophobic intermediate layers and evaluation of gas permeation in the presence of water vapor. Journal of Membrane Science, 2015, 496, 156-164.	8.2	24
46	Tailoring the Subnano Silica Structure via Fluorine Doping for Development of Highly Permeable CO ₂ Separation Membranes. ChemNanoMat, 2016, 2, 264-267.	2.8	24
47	Fabrication and Microstructure Tuning of a Pyrimidine-Bridged Organoalkoxysilane Membrane for CO ₂ Separation. Industrial & Engineering Chemistry Research, 2017, 56, 1316-1326.	3.7	24
48	Selective water vapor permeation from steam/non-condensable gas mixtures via organosilica membranes at moderate-to-high temperatures. Journal of Membrane Science, 2019, 589, 117254.	8.2	24
49	Development of high-performance sub-nanoporous SiC-based membranes derived from polytitanocarbosilane. Journal of Membrane Science, 2020, 598, 117688.	8.2	24
50	Amino-decorated organosilica membranes for highly permeable CO2 capture. Journal of Membrane Science, 2020, 611, 118328.	8.2	24
51	Tailoring the Separation Behavior of Polymer-Supported Organosilica Layered-Hybrid Membranes via Facile Post-Treatment Using HCl and HN ₃ Vapors. ACS Applied Materials & Interfaces, 2016, 8, 11060-11069.	8.0	23
52	Microporous Nickel-Coordinated Aminosilica Membranes for Improved Pervaporation Performance of Methanol/Toluene Separation. ACS Applied Materials & amp; Interfaces, 2021, 13, 23247-23259.	8.0	23
53	Enhanced CO 2 separation performance for tertiary amineâ€silica membranes via thermally induced local liberation of CH 3 Cl. AICHE Journal, 2018, 64, 1528-1539.	3.6	22
54	Preparation and gas permeation properties of thermally stable organosilica membranes derived by hydrosilylation. Journal of Materials Chemistry A, 2014, 2, 672-680.	10.3	21

#	Article	IF	CITATIONS
55	Nanofiltration performance of SiO2-ZrO2 membranes in aqueous solutions at high temperatures. Separation and Purification Technology, 2016, 168, 238-247.	7.9	21
56	Pervaporation via siliconâ€based membranes: Correlation and prediction of performance in pervaporation and gas permeation. AICHE Journal, 2021, 67, e17223.	3.6	21
57	Dissolution rates of alkaline rocks by carbonic acid: Influence of solid/liquid ratio, temperature, and CO2 pressure. Chemical Engineering Research and Design, 2013, 91, 933-941.	5.6	20
58	Reverse osmosis performance of layered-hybrid membranes consisting of an organosilica separation layer on polymer supports. Journal of Membrane Science, 2015, 494, 104-112.	8.2	19
59	Development and permeation properties of SiO2-ZrO2 nanofiltration membranes with a MWCO of <200. Journal of Membrane Science, 2017, 535, 331-341.	8.2	19
60	Highâ€performance molecularâ€separation ceramic membranes derived from oxidative crossâ€linked polytitanocarbosilane. Journal of the American Ceramic Society, 2020, 103, 4473-4488.	3.8	19
61	Preparation and Gas Permeation Properties of Fluorine–Silica Membranes with Controlled Amorphous Silica Structures: Effect of Fluorine Source and Calcination Temperature on Network Size. ACS Applied Materials & Interfaces, 2017, 9, 24625-24633.	8.0	18
62	Al2O3 nanofiltration membranes fabricated from nanofiber sols: Preparation, characterization, and performance. Journal of Membrane Science, 2020, 611, 118401.	8.2	18
63	Microstructure evolution and enhanced permeation of SiC membranes derived from allylhydridopolycarbosilane. Journal of Membrane Science, 2020, 612, 118392.	8.2	18
64	Facile and Scalable Flow-Induced Deposition of Organosilica on Porous Polymer Supports for Reverse Osmosis Desalination. ACS Applied Materials & Interfaces, 2018, 10, 14070-14078.	8.0	17
65	High-temperature stability of PECVD-derived organosilica membranes deposited on TiO2 and SiO2–ZrO2 intermediate layers using HMDSO/Ar plasma. Separation and Purification Technology, 2014, 121, 13-19.	7.9	16
66	Hydrothermal stability and permeation properties of TiO2-ZrO2 (5/5) nanofiltration membranes at high temperatures. Separation and Purification Technology, 2019, 212, 1001-1012.	7.9	16
67	Metal-induced microporous aminosilica creates a highly permeable gas-separation membrane. Materials Chemistry Frontiers, 2021, 5, 3029-3042.	5.9	16
68	Ultrafast Synthesis of Silica-Based Molecular Sieve Membranes in Dielectric Barrier Discharge at Low Temperature and Atmospheric Pressure. Journal of the American Chemical Society, 2021, 143, 35-40.	13.7	16
69	Sol–gel spin coating process to fabricate a new type of uniform and thin organosilica coating on polysulfone film. Materials Letters, 2013, 109, 130-133.	2.6	15
70	Organosilica bis(triethoxysilyl)ethane (BTESE) membranes for gas permeation (GS) and reverse osmosis (RO): The effect of preparation conditions on structure, and the correlation between gas and liquid permeation properties. Journal of Membrane Science, 2017, 526, 242-251.	8.2	15
71	A carbon–silica–zirconia ceramic membrane with CO ₂ flow-switching behaviour promising versatile high-temperature H ₂ /CO ₂ separation. Journal of Materials Chemistry A, 2020, 8, 23563-23573.	10.3	15
72	Tuning the microstructure of polycarbosilane-derived SiC(O) separation membranes via thermal-oxidative cross-linking. Separation and Purification Technology, 2020, 248, 117067.	7.9	15

#	Article	IF	CITATIONS
73	Pore subnano-environment engineering of organosilica membranes for highly selective propylene/propane separation. Journal of Membrane Science, 2020, 603, 117999.	8.2	15
74	Development of an acetylacetonate-modified silica-zirconia composite membrane applicable to gas separation. Journal of Membrane Science, 2020, 599, 117844.	8.2	15
75	TiO ₂ Coatings Via Atmospheric-Pressure Plasma-Enhanced Chemical Vapor Deposition for Enhancing the UV-Resistant Properties of Transparent Plastics. ACS Omega, 2021, 6, 1370-1377.	3.5	15
76	Pore size tuning of sol-gel-derived triethoxysilane (TRIES) membranes for gas separation. Journal of Membrane Science, 2017, 524, 64-72.	8.2	14
77	Tailoring the molecular sieving properties and thermal stability of carbonized membranes containing polyhedral oligomeric silsesquioxane (POSS)-polyimide via the introduction of norbornene. Journal of Membrane Science, 2019, 582, 59-69.	8.2	14
78	Fineâ€ŧuned, molecularâ€composite, organosilica membranes for highly efficient propylene/propane separation via suitable pore size. AICHE Journal, 2020, 66, e16850.	3.6	14
79	Improved performance of organosilica membranes for steam recovery at moderate-to-high temperatures via the use of a hydrothermally stable intermediate layer. Journal of Membrane Science, 2021, 620, 118895.	8.2	13
80	A closer look at the development and performance of organic–inorganic membranes using 2,4,6-tris[3(triethoxysilyl)-1-propoxyl]-1,3,5-triazine (TTESPT). RSC Advances, 2014, 4, 12404.	3.6	12
81	Tailoring a Thermally Stable Amorphous SiOC Structure for the Separation of Large Molecules: The Effect of Calcination Temperature on SiOC Structures and Gas Permeation Properties. ACS Omega, 2018, 3, 6369-6377.	3.5	12
82	Vapor-permeation dehydration of isopropanol using a flexible and thin organosilica membrane with high permeance. Journal of Membrane Science, 2019, 588, 117226.	8.2	12
83	Chemical-free cleaning of fouled reverse osmosis (RO) membranes derived from bis(triethoxysilyl)ethane (BTESE). Journal of Membrane Science, 2020, 601, 117919.	8.2	12
84	Reverse osmosis and pervaporation of organic liquids using organosilica membranes: Performance analysis and predictions. AICHE Journal, 2022, 68, .	3.6	12
85	Nanogradient Hydrophilic/Hydrophobic Organosilica Membranes Developed by Atmospheric-Pressure Plasma to Enhance Pervaporation Performance. ACS Nano, 2022, 16, 10302-10313.	14.6	12
86	Pore size control of Al-doping into bis (triethoxysilyl) methane (BTESM)-derived membranes for improved gas permeation properties. RSC Advances, 2013, 3, 12080.	3.6	11
87	Preparation of cyclic peptide nanotube structures and molecular simulation of water adsorption and diffusion. Journal of Membrane Science, 2017, 537, 101-110.	8.2	11
88	Ceramic-Supported Polyhedral Oligomeric Silsesquioxane–Organosilica Nanocomposite Membrane for Efficient Gas Separation. Industrial & Engineering Chemistry Research, 2019, 58, 21708-21716.	3.7	11
89	Evaluation of experimentally obtained permeance based on module simulation: How should permeance be evaluated?. AICHE Journal, 2020, 66, e16250.	3.6	11
90	Experimental study and modeling of organic solvent reverse osmosis separations through organosilica membranes. AICHE Journal, 2020, 66, e16283.	3.6	11

#	Article	IF	CITATIONS
91	Hydrocarbon permeation properties through microporous fluorine-doped organosilica membranes with controlled pore sizes. Journal of Membrane Science, 2021, 619, 118787.	8.2	11
92	Enhanced production of butyl acetate via methanol-extracting transesterification membrane reactors using organosilica membrane: Experiment and modeling. Chemical Engineering Journal, 2022, 429, 132188.	12.7	11
93	Structural two-phase evolution of aminosilica-based silver-coordinated membranes for increased hydrogen separation. Journal of Membrane Science, 2022, 642, 119962.	8.2	11
94	Poreâ€size evaluation and gas transport behaviors of microporous membranes: An experimental and theoretical study. AICHE Journal, 2015, 61, 2268-2279.	3.6	10
95	Photo-induced sol–gel processing for low-temperature fabrication of high-performance silsesquioxane membranes for use in molecular separation. Chemical Communications, 2015, 51, 9932-9935.	4.1	10
96	Plasma-assisted multi-layered coating towards improved gas permeation properties for organosilica membranes. RSC Advances, 2015, 5, 59837-59844.	3.6	10
97	Atmospheric-Pressure Plasma-Enhanced Chemical Vapor Deposition of Hybrid Silica Membranes. Journal of Chemical Engineering of Japan, 2018, 51, 732-739.	0.6	10
98	Structural transformation of the nickel coordination-induced subnanoporosity of aminosilica membranes for methanol-selective, high-flux pervaporation. Journal of Membrane Science, 2022, 656, 120613.	8.2	10
99	Molecular dynamics simulation study on characterization of bis(triethoxysilyl)-ethane and bis(triethoxysilyl)ethylene derived silica-based membranes. Desalination and Water Treatment, 2013, 51, 5248-5253.	1.0	9
100	Micropore Filling Phase Permeation of a Condensable Vapor in Silica Membranes: A Molecular Dynamics Study. Journal of Chemical Engineering of Japan, 2013, 46, 659-671.	0.6	9
101	Tuning the pore sizes of novel silica membranes for improved gas permeation properties via an in situ reaction between NH ₃ and Si–H groups. Chemical Communications, 2015, 51, 2551-2554.	4.1	9
102	Plasma treatment of hydrophobic sub-layers to prepare uniform multi-layered films and high-performance gas separation membranes. Applied Surface Science, 2015, 349, 415-419.	6.1	9
103	Acid post-treatment of sol-gel-derived ethylene-bridged organosilica membranes and their filtration performances. Journal of Membrane Science, 2018, 556, 196-202.	8.2	9
104	SiC mesoporous membranes for sulfuric acid decomposition at high temperatures in the iodine–sulfur process. RSC Advances, 2020, 10, 41883-41890.	3.6	9
105	Evaluating the gas permeation properties and hydrothermal stability of organosilica membranes under different hydrosilylation conditions. Journal of Membrane Science, 2015, 493, 664-672.	8.2	8
106	TiO2-ZrO2 membranes of controlled pore sizes with different Ti/Zr ratios for nanofiltration. Journal of Sol-Gel Science and Technology, 2019, 92, 12-24.	2.4	8
107	Pore size tuning of bis(triethoxysilyl)propane (BTESP)-derived membrane for gas separation: Effects of the acid molar ratio in the sol and of the calcination temperature. Separation and Purification Technology, 2020, 242, 116742.	7.9	8
108	Phosphorus Recovery from Wastewater Treatment Plants by Using Waste Concrete. Journal of Chemical Engineering of Japan, 2011, 44, 48-55.	0.6	8

HIROKI NAGASAWA

#	Article	IF	CITATIONS
109	Ammonia permeation of fluorinated sulfonic acid polymer/ceramic composite membranes. Journal of Membrane Science, 2022, 658, 120718.	8.2	8
110	Propylene/propane Permeation Properties of Metal-doped Organosilica Membranes with Controlled Network Sizes and Adsorptive Properties. Journal of the Japan Petroleum Institute, 2016, 59, 140-148.	0.6	7
111	Hydrothermal stability of fluorineâ€induced microporous silica membranes: Effect of steam treatment conditions. AICHE Journal, 2021, 67, e17292.	3.6	7
112	Facile low-temperature route toward the development of polymer-supported silica-based membranes for gas separation via atmospheric-pressure plasma-enhanced chemical vapor deposition. Journal of Membrane Science, 2021, 638, 119709.	8.2	7
113	Evaluation of non-commercial ceramic SiO2-ZrO2 and organosilica BTESE membranes in a highly oxidative medium: Performance in hydrogen peroxide. Journal of Membrane Science, 2016, 520, 740-748.	8.2	6
114	Evaluating the chemical stability of metal oxides in SO 3 and applications of SiO 2 â€based membranes to O 2 /SO 3 separation. Journal of the American Ceramic Society, 2019, 102, 6946-6956.	3.8	6
115	Molecular dynamics simulation study on the mechanisms of liquid-phase permeation in nanopores. Separation and Purification Technology, 2019, 220, 259-267.	7.9	6
116	Design of a SiOC network structure with oxidation stability and application to hydrogen separation membranes at high temperatures. Journal of Membrane Science, 2021, 625, 119147.	8.2	6
117	Phosphorus Recovery from Wastewater Treatment Plant by Using Waste Concretes. Kagaku Kogaku Ronbunshu, 2009, 35, 12-19.	0.3	6
118	Enhancement of the H2-permselectivity of a silica-zirconia composite membrane enabled by ligand-ceramic to carbon-ceramic transformation. Journal of Membrane Science, 2022, 642, 119948.	8.2	6
119	Microporous structure control of SiO2-ZrO2 composite membranes via Yttrium doping and an evaluation of thermal stability. Journal of Sol-Gel Science and Technology, 2022, 104, 566-579.	2.4	6
120	Photo-induced sol–gel synthesis of polymer-supported silsesquioxane membranes. RSC Advances, 2017, 7, 7150-7157.	3.6	5
121	Correlation Between Ammonia Selectivity and Temperature Dependent Functional Group Tuning of GO. IEEE Nanotechnology Magazine, 2021, 20, 129-136.	2.0	5
122	Steam recovery via nanoporous and subnanoporous organosilica membranes: The effects of pore structure and operating conditions. Separation and Purification Technology, 2021, 275, 119191.	7.9	5
123	Controlled organosilica networks via metal doping for improved dehydration membranes with layered hybrid structures. Separation and Purification Technology, 2021, 278, 119561.	7.9	5
124	Open-air plasma deposition of polymer-supported silica-based membranes for gas separation. Separation and Purification Technology, 2022, 291, 120908.	7.9	5
125	Plasma-enhanced chemical vapor deposition of amorphous carbon molecular sieve membranes for gas separation. RSC Advances, 2016, 6, 59045-59049.	3.6	4

Silica Membrane Application for Pervaporation Process. , 2017, , 217-241.

#	Article	IF	CITATIONS
127	Effects of Calcination Condition on the Network Structure of Triethoxysilane (TRIES) and How Si–H Groups Influence Hydrophobicity Under Hydrothermal Conditions. Industrial & Engineering Chemistry Research, 2019, 58, 3867-3875.	3.7	4
128	Effect of the Ti/Zr ratio on the hydrothermal and chemical stability of TiO2-ZrO2 nanofiltration membranes. Separation and Purification Technology, 2021, 274, 119060.	7.9	4
129	Network tailoring of organosilica membranes <i>via</i> aluminum doping to improve the humid-gas separation performance. RSC Advances, 2022, 12, 5834-5846.	3.6	4
130	Tailoring the structure of a sub-nano silica network via fluorine doping to enhance CO2 separation and evaluating CO2 separation performance under dry or wet conditions. Journal of Membrane Science, 2022, 658, 120735.	8.2	4
131	Pore Structure Controllability and CO2 Permeation Properties of Silica-Derived Membranes with a Dual-Network Structure. Industrial & Engineering Chemistry Research, 2021, 60, 8527-8537.	3.7	3
132	Effect of fluorine doping on the network pore structure of non-porous organosilica bis(triethoxysilyl)propane (BTESP) membranes for use in molecular separation. Journal of Membrane Science, 2022, 644, 120083.	8.2	3
133	Preliminary techno-economic analysis of non-commercial ceramic and organosilica membranes for hydrogen peroxide ultrapurification. Chemical Engineering Research and Design, 2017, 125, 385-397.	5.6	2
134	Free glycerol removal from monoglyceride using TiO2-ZrO2 nanofiltration membranes. Separation and Purification Technology, 2019, 224, 366-372.	7.9	2
135	Facile development of microstructure-engineered, ligand-chelated SiO2–ZrO2 composite membranes for molecular separations. Molecular Systems Design and Engineering, 2021, 6, 429-444.	3.4	2
136	Atmospheric-pressure PECVD synthesis of polymer-supported molecular sieving silica membranes for gas separation: Effect of pore size of polymeric support. Materials Letters, 2021, , 131211.	2.6	2
137	Design of carbon–ceramic composite membranes with tunable molecular cut-offs from a carboxylic benzoxazine ligand chelated to silica–zirconia. Molecular Systems Design and Engineering, 0, , .	3.4	2
138	Hydrophilic behavior of methyl-terminated organosilica thin films modified by atmospheric-pressure water vapor plasma. Materials Letters, 2022, 325, 132841.	2.6	2
139	Transesterification membrane reactor with organosilica membrane in batch and continuous flow modes. Chemical Engineering Journal, 2022, 450, 137862.	12.7	2
140	Effect of Sintering Temperature on Sol–Gel Synthesis of Porous Polymeric Membrane Supported Layered Hybrid Organosilica Membranes and Their Vapor Permeation Property. Kagaku Kogaku Ronbunshu, 2019, 45, 177-183.	0.3	1
141	Treatment of Oily Wastewater by Ceramic Membranes. Membrane, 2020, 45, 35-40.	0.0	1
142	Infrared-spectroscopic porosimetry: Development and application for characterization of hundred-nanometer-thick porous thin films. Thin Solid Films, 2019, 685, 299-305.	1.8	0
143	Chemical Vapor Deposition. , 2016, , 395-397.		0
144	Nano/subnano-tuning of Porous Silica Membranes and Application to Hydrogen Separation. Membrane, 2018, 43, 180-187.	0.0	0

#	Article	IF	CITATIONS
145	Atmospheric–pressure Plasma–enhanced CVD of Hybrid Silica Membranes at Ambient Temperature and Pressure. Membrane, 2019, 44, 10-15.	0.0	О